

RESEARCH ARTICLE

Curcumin-loaded PLGA Nanoparticles Conjugated with Anti-P-glycoprotein Antibody to Overcome Multidrug Resistance

Wanisa Punfa^{1,2}, Shugo Suzuki², Pornsiri Pitchakarn¹, Supachai Yodkeeree¹, Taku Naiki², Satoru Takahashi², Pornngarm Limtrakul^{1*}

Abstract

Background: The encapsulation of curcumin (Cur) in polylactic-co-glycolic acid (PLGA) nanoparticles (Cur-NPs) was designed to improve its solubility and stability. Conjugation of the Cur-NPs with anti-P-glycoprotein (P-gp) antibody (Cur-NPs-APgp) may increase their targeting to P-gp, which is highly expressed in multidrug-resistance (MDR) cancer cells. This study determined whether Cur-NPs-APgp could overcome MDR in a human cervical cancer model (KB-V1 cells) *in vitro* and *in vivo*. **Materials and Methods:** First, we determined the MDR-reversing property of Cur in P-gp-overexpressing KB-V1 cells *in vitro* and *in vivo*. Cur-NPs and Cur-NPs-APgp, in the range 150-180 nm, were constructed and subjected to an *in vivo* pharmacokinetic study compared with Cur. The *in vitro* and *in vivo* MDR-reversing properties of Cur-NPs and Cur-NPs-APgp were then investigated. Moreover, the stability of the NPs was determined in various solutions. **Results:** The combined treatment of paclitaxel (PTX) with Cur dramatically decreased cell viability and tumor growth compared to PTX treatment alone. After intravenous injection, Cur-NPs-APgp and Cur-NPs could be detected in the serum up to 60 and 120 min later, respectively, whereas Cur was not detected after 30 min. Pretreatment with Cur-NPs-APgp, but not with NPs or Cur-NPs, could enhance PTX sensitivity both *in vitro* and *in vivo*. The constructed NPs remained a consistent size, proving their stability in various solutions. **Conclusions:** Our functional Cur-NPs-APgp may be a suitable candidate for application in a drug delivery system for overcoming drug resistance. The further development of Cur-NPs-APgp may be beneficial to cancer patients by leading to its use as either as a MDR modulator or as an anticancer drug.

Keywords: Multidrug resistance - curcumin - nanoparticles - targeting drug delivery

Asian Pac J Cancer Prev, 15 (21), 9249-9258

Introduction

Multidrug resistance (MDR) is a major problem for the success of cancer chemotherapy and is closely associated with treatment failure in the most common forms of cancer, including lung, colon, breast, and cervical cancer (Chang, 2003). Overexpression of P-glycoprotein (P-gp), a 170-kDa plasma membrane transporter, has been identified as one of the major causes of drug resistance in several cancers. P-gp belongs to the superfamily of ATP-binding cassette (ABC) transporters (Chang, 2003) that act as an ATP-dependent efflux pump and has a broad substrate specificity that includes xenobiotics (Bain et al., 1997), etoposide (Burgio et al., 1998), doxorubicin (Shen et al., 2008), vinblastine (Cisternino et al., 2004), and paclitaxel (PTX) (Jang et al., 2001; Gallo et al., 2003). Increased expression of P-gp, the product of the human MDR1 gene, is a well-characterized mechanism used by cancer cells to avoid the cytotoxic action of anticancer drugs. Based on decreases in intracellular drug accumulation by P-gp,

studies of the MDR gene promoter sequence suggest that modulation of P-gp expression at the genetic level may be a possible way to overcome MDR (Hu et al., 1996).

Curcumin (Cur), a phenolic compound purified from the rhizome of *Curcuma longa*, has a long history of being used in traditional medicine (Oyagbemi et al., 2009; Dai et al., 2013). Recently, Cur has been reported to reduce both the expression and function of P-gp (Anuchapreeda et al., 2002; Limtrakul et al., 2004). The safety of *Curcuma longa* and its derivatives has been demonstrated in various animal models (Qureshi et al., 1992), and it is clear that turmeric is not toxic in humans even at high doses (12 g/day) (Anand et al., 2007). Thus, Cur could be considered a promising lead compound in the design of more effective MDR chemosensitizers by inhibiting P-gp function and/or expression (Qureshi et al., 1992). Previous studies have reported that a combined treatment of vincristine with Cur reduced tumor growth in a colon cancer xenograft model. However, an *in vivo* study using a combination treatment of PTX with Cur against human MDR cervical

¹Department of Biochemistry, Faculty of Medicine, Chiang Mai University, Chiang Mai, Thailand, ²Department of Experimental Pathology and Tumor Biology Graduate School of Medical Science, Nagoya City University, Nagoya, Japan *For correspondence: pornngarm.d@cmu.ac.th

carcinoma cells (KB-V1) has never been reported. This study has therefore evaluated the combined treatment of PTX and Cur *in vivo*.

Because the efficacy of Cur is limited due to the low level of oral bioavailability, poor absorption ability, a high metabolic rate, inactivity of metabolic products together with rapid elimination and clearance from the body (Anand et al., 2007), poor pharmacokinetics (Shehzad et al., 2010) and solubility, and degradation under natural to basic pH conditions, the development of Cur in clinical applications using nanoparticles (NPs) as drug delivery systems (DDS) has been suggested to address these issues. To overcome the challenges of targeting tumors with nanotechnology, it is important to combine the rational design of nanocarriers or nanoparticles (Yin et al., 2013; Yadav et al., 2014) with a fundamental understanding of tumor biology by considering the general characteristics of tumors, which include poor lymphatic drainage, the overexpression of vascular endothelial growth factors, and leaky blood vessels. Recently, passive-targeting nanocarriers have been developed that can extravasate into tumor tissues via leaky vessels by the enhanced permeability and retention (EPR) effect. However, free drugs that diffuse non-specifically are traditionally those that have been studied and of interest (Maeda et al., 2000).

However, the passive targeting process still has many limitations. Targeting cells within a tumor is not always possible because some drugs do not diffuse efficiently, and the random nature of the approach makes it difficult to control the process. One approach to overcome these limitations is to program the NPs to actively bind to specific cells after extravasation. This binding may be achieved by attaching targeting agents, such as ligands, antibodies or peptides to the surface of the NPs by a variety of conjugation chemistries (Torchilin, 2005). The NPs will therefore recognize and bind to the target cells through ligand-receptor interactions, and the bound carriers are then internalized before the drug is released inside the cells.

In general, when using a targeting agent to deliver NPs to the cancer cells, it is imperative that the agent binds with high selectivity to the molecules that are uniquely expressed on the cell surface. A previous study showed that combined products that are associated with PTX should be encapsulated into the polymeric NPs to avoid a solubility issue with the surface coating. In addition, the use of anti-HER2 antibody as a recognition ligand for ovarian cancer cells resulted in a significant improvement of anticancer activity in a disseminated xenograft ovarian cancer model (Cirstoiu-Hapca et al., 2010).

In our previous study, we generated Cur entrapped in polymeric NPs consisting of poly (DL-lactide-co-glycolic acid) (PLGA) (Tabatabaei Mirakabad et al., 2014); these biodegradable and biocompatible polymers are therapeutic devices approved by the Food and Drug Administration (FDA) (Makadia and Siegel, 2011). We observed that the cellular uptake and cytotoxicity of Cur were increased in KB-V1 cells using NP-loading. Interestingly (Punfa et al., 2012), the conjugation of Cur-loaded NPs with anti-P-gp antibody (APgp) (Cur-NPs-APgp) induced a higher cytotoxicity rate than Cur-loaded NPs (Cur-NPs) in

KB-V1 cells *in vitro* (Punfa et al., 2012). Therefore, P-gp should be considered a target molecule in MDR cancers.

In the present study, we considered the additive effects of Cur-NPs-APgp on treatments using PTX, one of the drugs of choice for cervical cancer chemotherapy (Qiao et al., 2011). First, we determined the *in vitro* and *in vivo* MDR-reversing properties of Cur in P-gp-overexpressing human cervical cancer cells (KB-V1). Cur-NPs and Cur-NPs-APgp were constructed and subjected to *in vivo* pharmacokinetic analysis to determine the Cur remaining in the serum after an intravenous (i.v.) injection of Cur, Cur-NPs and Cur-NPs-APgp. Finally, the *in vitro* and *in vivo* MDR-reversing properties of Cur, Cur-NPs and Cur-NPs-APgp were then determined in KB-V1 (drug-resistant cervical cancer) cells, KB-3-1 (drug-sensitive cervical cancer) cells and a KB-V1 xenograft model.

Materials and Methods

Mouse monoclonal anti-P-glycoprotein (P-gp) antibody (APgp; clone F4), Poly (DL-lactide-co-glycolide) (PLGA; lactide to glycolide ratio 50:50), N-(3-dimethylaminopropyl)-N'-ethylcarbodiimide hydrochloride (EDC), N-hydroxysuccinimide (NHS) and Pluronic F-127 (Ploxamer 407) were purchased from Sigma-Aldrich (St. Louis, MO, USA), 4-Dimethylaminopyridine (DMAP) and succinic anhydride were purchased from Fluka Chemie GmbH (Buchs, Switzerland). Dulbecco's modified Eagle's medium, penicillin-streptomycin, fetal bovine serum (FBS) and 0.05% trypsin-EDTA were purchased from Life Technologies Corp. (Carlsbad, CA, USA). Triethylamine and Amicon Ultra-4 centrifugal Filter Devices (30K) were supplied by Merck KGaA (Darmstadt, Germany). Acetone, tetrahydrofuran (THF), chloroform, dimethyl sulfoxide (DMSO), methanol (HPLC grade), acetonitrile (HPLC grade) and diethyl ether were purchased from Wako Pure Chemical Industries, Ltd. (Osaka, Japan). Ki-67 antibody (clone SP6) was purchased from Acris Antibodies GmbH (Herford, Germany). Terminal deoxynucleotidyl transferase-mediated dUTP nick-end labeling (TUNEL) assay was performed using an In Situ Apoptosis Detection Kit from Takara (Otsu, Japan).

Cell cultures

The multidrug resistant (KB-V1) and drug sensitive (KB-3-1) cervical carcinoma cell (Anuchapreeda et al., 2002; Chearwae et al., 2004) lines were generous gifts from Dr. Michael M. Gottesman (National Cancer Institute, Bethesda, MD). Both cell lines were cultured in DMEM with 10% FBS, 2 mM L-glutamine, 50 U/mL penicillin, and 50 µg/mL streptomycin, and 1 µg/mL of vinblastine was added only to the KB-V1 culture medium. The cells were maintained in a humidified incubator at 37°C with an atmosphere containing 5% CO₂. The expression of P-gp in KB-V1 and KB-3-1 cells was confirmed by western blot analysis, as described previously (Chearwae et al., 2004; Limtrakul et al., 2004).

Animals

All animal experiments were performed under

protocols approved by the Institutional Animal Care and Use Committee of Nagoya City University Graduate School of Medical Sciences, which were based on the International Guiding Principles for Biomedical Research Involving Animals published in 1985 CIOMS (1985).

Seven-week-old female BALB/c mice and 9-week-old female BALB/c-nu/nu mice were purchased from Charles River Japan Inc. (Atsugi, Japan) and housed in plastic cages with hardwood chip bedding in an air-conditioned room at 23±2°C, and 55±5% humidity with a 12 h light/dark cycle. An Oriental MF diet (Oriental MF, Oriental Yeast Co., Tokyo, Japan) and distilled water were available ad libitum.

Effect of Cur on PTX sensitivity in KB-V1 cells

The effect of Cur on PTX sensitivity in KB-V1 cells was performed to determine the MDR-reversing property of Cur. The cells (1,000 cells/well) were seeded in 96-well plates for 24 h. Next, DMEM medium with fetal bovine serum containing Cur (5 or 7.5 µM each well) and various doses of PTX (0-2.5 µM) were added and incubated for 48 h. After the treatment, MTT dye (15 µL, 5 mg/mL) was added and incubated for an additional 4 h. The absorbance of each well was measured using a microplate reader at 540 nm with a reference wavelength of 630 nm.

Effect of Cur on PTX sensitivity in a KB-V1 xenograft model

To examine the MDR-reversing property of Cur on PTX sensitivity in a KB-V1 xenograft model, 10-week old female BALB/c-nu/nu mice were administered KB-V1 cells (1×10⁷ cells) subcutaneously in the rear area of mice. As soon as the tumor volume reached approximately 100 mm³ in sizes, the mice were divided into 2 groups (PTX and PTX+Cur), each containing 10 mice per group. For the pretreatment, mice were i.v. injected with the vehicle control (3% DMSO and 1% Tween-20 in saline) and Cur at a dose of 10 mg/kg body weight. Thirty minutes after the injection, mice were administered paclitaxel (3 mg/kg body weight) by intraperitoneal (i.p.) injection. These treatments were administered once per week for 3 weeks.

The body weight was measured three times a week. Mice were euthanized at experimental week 4 and then primary tumors, liver, lungs, kidneys, spleen and lymph nodes were removed. Primary tumors were measured and the tumor volume was calculated using the following formula: 0.52 (axis 1 × axis 2 × axis 3). The tumor and other organs were fixed in 10% buffered formalin. A minimum of 1 section of each tissue and the largest section from each lobe of the lung were processed for hematoxylin and eosin (H&E) staining. The tumor sections were subjected to a TUNEL assay and immunostaining.

TUNEL assays

Paraffin-embedded specimens were sectioned and apoptotic cells in the tumor tissue were detected using a TUNEL assay. The TUNEL assay was performed using an *in situ* Apoptosis Detection Kit according to the manufacturer's instructions. The number of TUNEL-labeled cells in a minimum of 1000 cells was counted to determine the labeling index.

Immunohistochemistry for Ki-67 staining

Paraffin-embedded specimens were sectioned and stained with antibodies against Ki-67, a marker of cell proliferation. The sections were then stained sequentially with secondary antibodies and an avidin-biotin complex. The binding sites were visualized with diaminobenzidine. The sections were counterstained lightly with hematoxylin and eosin for microscopic examination. The number of Ki-67-labeled cells in a minimum of 1000 tumor cells was counted to determine a labeling index.

Preparation of Cur-encapsulated PLGA nanoparticles (Cur-NPs) for *in vivo* study

Cur-NPs were prepared using the nanoprecipitation technique (Iangcharoen et al., 2011; Punfa et al., 2012). Briefly, PLGA (700 mg) was dissolved in 75 mL acetone containing 7 mg of Cur. Poloxamer-COOH (1,400 mg) was dissolved in 100 mL of deionized (DI) water. Then, the PLGA solution was drop-wise added into the poloxamer solution under overnight stirring. The NPs were then washed twice with DI water by centrifugation using the Amicon filtration device with a 30 kDa molecular weight cutoff membrane at 4,500 rpm for 50 min at 4°C to obtain Cur-NPs. The resulting nanoparticles were resuspended in DI water.

Preparation of APgp-conjugated Cur-NPs (Cur-NPs-APgp) for *in vivo* study

Cur-NPs were conjugated to APgp through the carbodiimide reaction (Punfa et al., 2012). Briefly, the Cur-NPs were adjusted to pH 5.8, then incubated with the appropriate amount of NHS (50 mM) and EDC (100 mM) for 30 min. One milliliter of PBS was added to the NPs at a pH of 7.4 and 50 µL of APgp was added under gentle stirring. The solution was then incubated overnight. Cur-NPs-APgp was collected by centrifugation at 12,000 rpm for 15 min at 4°C and resuspended with DI water.

Characterization of the NPs and determination of % entrapment efficiency and loading content of Cur

Mean diameter, zeta potential, and particle distribution (polydispersity index) of the NPs were characterized by photon correlation spectroscopy (PCS) (Zetasizer, Malvern Instrument, UK). The entrapment efficiency and loading content of Cur were determined by direct method using a UV-visible spectrophotometer. Fifty microliters of the NPs was dissolved with acetonitrile: DMSO (1:1) and measured using a UV-visible spectrophotometer at 425 nm for a determination of the Cur concentration. The concentration of Cur was calculated using the standard curve of Cur (1-10 µg/mL) in acetonitrile:DMSO (1:1). The Cur loading content and % entrapment efficiency were calculated as follows:

$$\% \text{ Entrapment efficiency} = \frac{\text{Amount of Curcumin in nanoparticles}}{\text{Amount of Curcumin added during nanoparticles preparation}} \times 100 \quad (1)$$

$$\text{Loading content} = \frac{\text{Amount of Cur in nanoparticles}}{1 \text{ mg of nanoparticles}} \quad (2)$$

Quantification of APgp on the surface of the NPs

The quantification of APgp on the surface of the NPs was evaluated by an indirect quantitation with a Bradford assay (Iangcharoen et al., 2011). The amount of APgp on the surface of the nanoparticles was calculated by subtracting the free amount of the sampling supernatant at the end of the centrifugation from the amount of sampling at the beginning before centrifugation took place. The standard curve was prepared from a 2 mg/mL stock of globulin over a concentration range of 0-25 µg/mL and was calculated as follows: $\%Ab\ conjugation = [(Protein\ in\ NP\ suspension - Protein\ in\ supernatant) \div Protein\ in\ NP\ suspension] \times 100$

In vivo pharmacokinetic study

The pharmacokinetic test of the NPs was evaluated using 8-week-old female BALB/c mice. The 48 mice were divided into 3 groups (Cur, Cur-NPs, and Cur-NPs-APgp). Mice were i.v. injected with Cur dissolved in 3% DMSO, 1% Tween-20 in saline, Cur-NPs or Cur-NPs-APgp, which were dissolved in DI water. The Cur concentration used in this experiment was adjusted to 10 mg/kg body weight of each mouse. After injection, mice were euthanized, and blood from each mouse was collected at 30, 60, 120 and 240 min (4 mice in each group). Liver and kidneys were removed and weighed. Part of the tissue was frozen for the determination of Cur concentration. The remaining tissue was fixed with 10% buffered formalin for histopathological examination.

HPLC (high-performance liquid chromatography) was performed for the determination of Cur concentration (Tsai et al., 2011) (Song et al., 2011). Fifty microliters of serum was mixed with trichloroacetic acid (1.5 mg/mL) in acetonitrile 100 µL and centrifuged at 12,000 rpm at 4°C for 20 minutes. Fifty microliters of the supernatant was collected and subjected to HPLC using a reversed-phase C18 column (WATER, MA, USA). The mobile phase was composed of 52% acetonitrile and 48% citric buffer (1% w/v citric acid solution adjusted to pH 3.0). The detection wavelength was 425 nm and the flow rate was set at 1.0 mL/min. The Cur concentration in the serum was calculated and compared to the standard curve of Cur (0-80 ng/mL).

Effect of Cur-NPs and Cur-NPs-APgp on PTX sensitivity in a KB-V1 xenograft model

To examine the MDR-reversing property of Cur-NPs and Cur-NPs-APgp on paclitaxel sensitivity using a KB-V1 xenograft model, 10-week old female BALB/c-nu/nu mice were administered KB-V1 cells (1×10^7 cells) subcutaneously in the rear area of the mice. As soon as the tumor volume reached approximately 100 mm³ in size, the mice were divided into 3 groups (PTX+NPs, PTX+Cur-NPs, and PTX+Cur-NPs-APgp), containing 10 mice per group. For the pretreatment, mice were i.v. injected with empty-NPs, Cur-NPs or Cur-NPs-APgp. The concentration of Cur was adjusted to 10 mg/kg body weight for each group. Thirty minutes after the injection, paclitaxel (3 mg/kg body weight) was administered to the mice by i.p. injection. These treatments were administered once per week for 3 weeks.

The body weight of each mouse was measured every week. Mice were euthanized at experimental week 4, and then primary tumors, liver, lungs, kidneys and lymph nodes were removed. Primary tumors were measured and the tumor volume was calculated using the following formula: $0.52 (axis\ 1 \times axis\ 2 \times axis\ 3)$. Sections of the primary tumor and other organs were fixed in 10% buffered formalin. A minimum of 1 section of each tissue, and the largest section from each lobe of the lung, were processed for H&E staining, immunostaining and a TUNEL assay.

Immunohistochemistry for F4/80 staining

Because we could detect macrophage accumulation in liver sinusoid sections stained with H&E, the tissue samples were subjected to immunohistochemistry using a specific antibody against the F4/80 antigen, a 160-kDa glycoprotein expressed by murine macrophages. Macrophages were counted under a microscope in 5 randomly selected areas (0.0625 mm² each) of the liver sections at a magnification of 400X (Yamate et al., 1993).

Effect of Cur-NPs and Cur-NPs-APgp on PTX sensitivity in KB-V1 and KB-3-1 cells

The pretreatment of Cur, Cur-NPs and Cur-NPs-APgp in KB-V1 and KB-3-1 cells followed by PTX was performed to study the effect of the NPs as a reversing agent of P-gp. The cells (1,000 cells/well) were seeded in 96-well plates for 24 h. Next, DMEM without fetal bovine serum containing Cur, Cur-NPs or Cur-NPs-APgp (the final concentration of Cur was 7.5 µM per well) was added and incubated for 6 h. The culture supernatant was subsequently removed and new media containing various concentrations of PTX (0-1 µM for KB-V1 cells and 0-1 nM for KB-3-1 cells) was added and incubated for another 42 h. NPs and NPs-APgp were used as vehicle controls. After the treatments, MTT dye (15 µL, 5 mg/mL) was added and incubated for 4 h. The absorbance of each well was measured using a microplate reader at 540 nm with a reference wavelength of 630 nm.

Stability testing of Cur-NPs and Cur-NPs-APgp

Testing of Cur-NPs and Cur-NPs-APgp was performed to investigate the stability of the mean diameter of the NPs over time (Lazzari et al., 2012). The NPs were diluted 1:10 (v/v) in various solutions including DI water, normal saline, phosphate buffer saline (PBS) pH 7.4 and pH 4.5 and incubated at 4°C for different times over a 5-day period. The mean diameter of the NPs was determined by photon correlation spectroscopy (PCS) every day for 5 days.

Statistical analysis

In the *in vivo* experiment, the data are presented as the mean±standard error of the mean (S.E.) values, and the data from the *in vitro* experiment are presented as the mean±standard deviation (S.D.) values. Statistical analysis was performed with Prism version 6.0 software using a t-test and one-way ANOVA, Dunnett's test or Tukey's multiple comparisons test, significance being determined at *p<0.05, **p<0.01, ***p<0.001 or ****p<0.0001.

Results

MDR modulation effect of Cur on PTX sensitivity in KB-V1 cells

The MDR-reversing property of Cur on PTX sensitivity in KB-V1 cells following a 48 h co-treatment of Cur (5 or 7.5 μM) and PTX significantly enhanced PTX-induced cell death compared with a single PTX treatment at each indicated concentration in KB-V1 cells (Figure 1). The IC_{50} value of the single PTX treatment was approximately 2 μM , while the IC_{50} value of the co-treatment with PTX (5 μM) and Cur (7.5 μM) was approximately 0.8 and 0.06 μM , respectively. Cur at concentrations of 5 and 7.5 μM could enhance the sensitivity of KB-V1 MDR cancer cells to PTX approximately 2.5- and 33.3-fold, respectively, compared to the single PTX treatment.

MDR modulation effect of Cur on PTX sensitivity using KB-V1 xenograft model

To determine the *in vivo* MDR-reversing property of Cur on PTX treatment, BALB/c-nu/nu mice were administered KB-V1 cells subcutaneously. After the tumor reached approximately 100 mm^3 in size, the mice were given the combined treatment of PTX with Cur (dissolved in 3% DMSO and 1% Tween-20 in saline) or PTX alone. The combined treatment of PTX with Cur markedly reduced the tumor size compared to the treatment of PTX alone, but did not reach statistical significance ($p=0.3621$), which may be due to the large margin of error (Figure 2A). To determine the anti-tumor effects of PTX combined with Cur, cell proliferation and apoptotic cells were calculated in the tumor sections (Figure 2B). The results showed that the number of apoptotic cells was dramatically increased in the combined treatment of PTX and Cur compared to the treatment of PTX alone, but was not significant ($p=0.1252$) (Figure 2C). However, there was no difference in the number of Ki-67-positive cells (Figure 2D).

Preparation and characterization of Cur-NPs and Cur-NPs-APgp

Cur-NPs and Cur-NPs-APgp were prepared using a modified nanoprecipitation technique as previously described (Punfa et al., 2012). For the *in vivo* study, the NPs were prepared in large quantity, 10 times more than

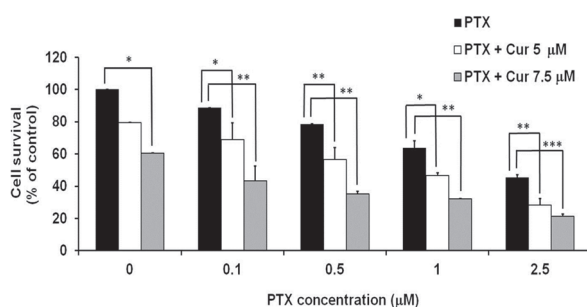


Figure 1. MDR Modulation Effect of Cur on PTX Sensitivity in KB-V1 Cells by Combined Treatment of PTX with Cur was Determined for 48 h. All assays were performed in triplicate and the mean \pm standard deviations are shown as * $p<0.05$, ** $p<0.01$ or *** $p<0.001$ versus PTX alone at each indicated concentration

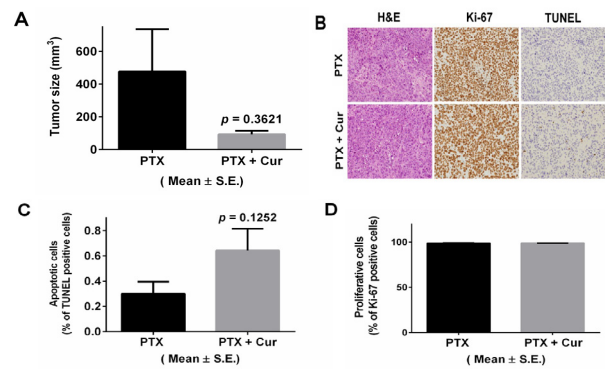


Figure 2. MDR Modulation Effect of Cur on PTX Sensitivity in a KB-V1 Xenograft Model was Examined.

For the combination treatment with PTX (3 mg/kg body weight) and Cur (10 mg/kg body weight), injections were performed once a week for 3 weeks. The tumors were weighed and the size was calculated at end of the study (A). TUNEL assay and Ki-67 were determined by immunohistochemistry (B) to detect the % TUNEL-positive cells (C) and % Ki-67 positive cells (D). All assays are represented as the mean \pm S.E

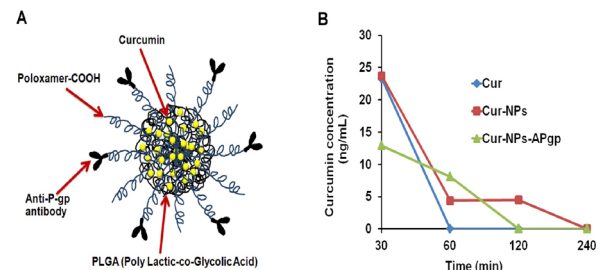


Figure 3. The Structure of Cur-NPs-APgp Composed of PLGA as a Carrier for the Entrapment of Cur, and Poloxamer-COOH as a Linker for Conjugation with APgp for the Specific Purpose of Targeting Tumor Cells (A).

The *in vivo* pharmacokinetic study showed the profile of Cur concentration in serum at the indicated times after i.v. injection with Cur, Cur-NPs or Cur-NPs-APgp (Cur 10 mg/kg body weight). The Cur concentration was determined by HPLC analysis (B)

for the *in vitro* study. Cur-NPs and Cur-NPs-APgp were completely dissolved in water. The structure of Cur-NPs-APgp was composed of PLGA as a carrier for the entrapment of Cur, and a poloxamer-COOH conjugated with APgp for active targeting to the P-gp on the surface of the cancer cells (Figure 3A). The mean diameter, polydispersity index (PDI), and zeta potential were calculated using PCS. The mean diameters of Cur-NPs and Cur-NPs-APgp were 162.3 and 165.4 nm, respectively. Moreover, both Cur-NPs and Cur-NP-APgp showed low polydispersity index, suggesting a narrow size distribution of the NPs. The zeta potential of Cur-NPs and Cur-NPs-APgp were -19.6 and -37.2 mV, respectively. The percent entrapment efficiency and loading content of Cur-NPs (60%, 11.9 μg Cur/mg NPs) were higher than for Cur-NPs-APgp (48%, 8.1 μg Cur/mg NPs). The percentage of anti-P-gp conjugation determined by the indirect method was 55.5% (Table 1).

In vivo pharmacokinetic study of Cur-NPs and Cur-NPs-APgp

The concentration of Cur in the serum at the indicated

Table 1. Physical Property of Cur-NPs and Cur-NPs-APgp Including Size, Polydispersity Index, Zeta Potential, % Entrapment Efficiency, Actual Loading and % Ab Conjugation

Characterization of NPs	Cur-NPs	Cur-NPs-APgp
Mean diameter (nm)	162.3±6.2	165.4±4.8
Polydispersity index (PDI)	0.096±0.032	0.093±0.017
Zeta potential (mV)	-19.6±2.3	-37.2±1.1
Entrapment efficiency (%)	60.0±5.0	48.0±1.7
Actual loading (μ g of Cur/mg NPs)	11.9±0.8	8.1±0.7
% Ab conjugation	-	55.5±3.7

*The data are presented as mean±standard deviation (S.D.) values

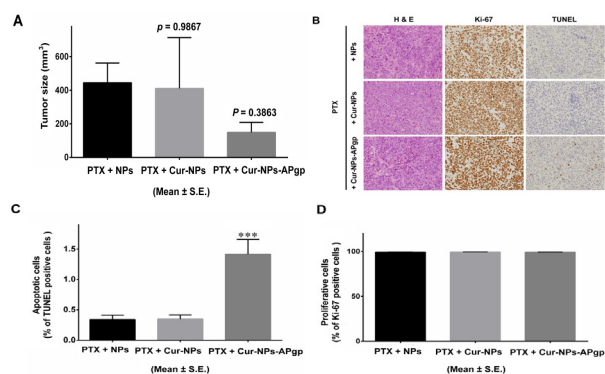


Figure 4. MDR Modulation Effect of Cur-NPs and Cur-NPs-APgp on PTX Sensitivity in a KB-V1 Xenograft Model was Examined. For the combined treatment of PTX (3 mg/kg body weight) and Cur-NPs or Cur-NPs-APgp (Cur 10 mg/kg body weight), injections were performed once a week for 3 weeks. The tumors were weighed and the size was calculated at end of the study (A). TUNEL assay and Ki-67 were determined by immunohistochemistry (B) to detect the % TUNEL-positive cells (C) and the %Ki-67-positive cells (D). All assays are represented as the mean±S.E (***) $p < 0.001$ versus PTX+NPs)

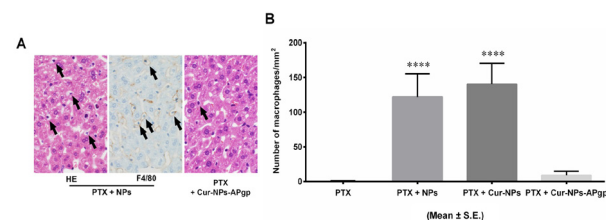


Figure 5. H&E Staining of the Liver Tissue Obtained from Mice that Received the Combined Treatment of PTX with Empty NPs, Cur-NPs or Cur-NPs-APgp Compared with PTX Alone, was Observed Under a Microscope (A). Macrophages were counted in the liver sinusoid, and the number of macrophages was calculated per square millimeter (B). All assays are represented as the mean±S.E (****) $p < 0.0001$ versus PTX)

times was determined by HPLC analysis (Figure 3B). Cur was detected in the serum of all groups (Cur, Cur-NPs, and Cur-NPs-APgp) 30 min after injection. The Cur concentration in groups treated with Cur, Cur-NPs, and Cur-NPs-APgp 30 min after injection was 23.3±9.6, 23.7±13.2 and 12.9±8.7 ng/ml, respectively. At 60 min after injection, Cur still remained in Cur-NP-treated (4.4±9.6 ng/ml) and the Cur-NP-APgp-treated (8.1±7.7 ng/ml) groups, but not in the Cur-treated group. While Cur was only detected in the Cur-NP-treated (4.5±4.2 ng/ml) group at 120 min, it was not detected at 240 min.

Cur was not detected in the liver and kidneys of all groups (data not shown).

MDR modulation effect of Cur-NPs and Cur-NPs-APgp on PTX sensitivity in a KB-V1 xenograft model

To determine the *in vivo* MDR-reversing property of Cur-NPs or Cur-NPs-APgp in the PTX treatment, BALB/c-nu/nu mice were administered KB-V1 cells subcutaneously. After the tumor reached approximately 100 mm³ in size, the mice were treated with the combined treatment of PTX with: 1) empty NPs; 2) Cur-NPs; or 3) Cur-NPs-APgp. No difference in body weight was observed among the groups during the experiment and at the time of euthanasia (data not shown). There were also no differences in organ weights among the groups (data not shown). The combined treatment of PTX and Cur-NPs-APgp decreased the tumor size by approximately one-fold when compared with the other groups, but this difference was not statistically significant due to the large margin of error ($p = 0.3863$) (Figure 4A). A TUNEL assay was used to determine a significant induction of apoptosis in the combined treatment of PTX with Cur-NPs-APgp compared to the combined treatment of PTX with empty NPs or with Cur-NPs (Figure 4B&C), whereas the number of Ki-67-positive cells was not different among all the groups (Figure 4B&D).

Macrophage detection in liver sinusoid

From microscopic observation of the H&E stained sections, macrophages were detected in the liver sinusoid of the PTX treatment with empty-NPs and Cur-NPs-treated groups (Figure 5A). To confirm the macrophages accumulation, immunostaining was performed using F4/80 antibodies that are specific for a 160-kDa glycoprotein expressed in murine macrophages (Figure 5A). The number of macrophages significantly increased in the PTX treatment with empty-NPs or Cur-NPs compared to the groups treated with Cur-NPs-APgp or PTX alone (Figure 5B). The treatment with NPs may induce macrophage accumulation, which may be involved in the elimination of the NPs remaining in the blood.

MDR modulation effect of Cur-NPs and Cur-NPs-APgp on the PTX sensitivity in KB-V1 and KB-3-1 cells

The modulation effect of Cur, Cur-NPs, Cur-NPs-APgp, NPs, and NPs-APgp on PTX sensitivity was determined in KB-V1 and KB-3-1 cells. Pretreatment with Cur-NPs-APgp, but not Cur, Cur-NPs or NPs (6 h), followed by PTX treatment (0.1-1 μ M) in KB-V1 cells significantly enhanced the PTX-induced cell death compared to PTX alone. The pretreatment of NPs-APgp, followed by PTX treatment (1 μ M) in KB-V1 cells did not enhance PTX-induced cell death, but a lower concentration (0.1-0.5 μ M) of the NPs-APgp pretreatment showed a significant difference from the control group (PTX alone). However, the pretreatment of Cur-NPs-APgp increased the efficacy and significantly increased the sensitivity of KB-V1 to PTX ($p < 0.05$) when compared to the NPs-APgp pretreatment (Figure 6A). In addition, there were no differences among the treatment groups in KB-3-1 cells (Figure 6B).

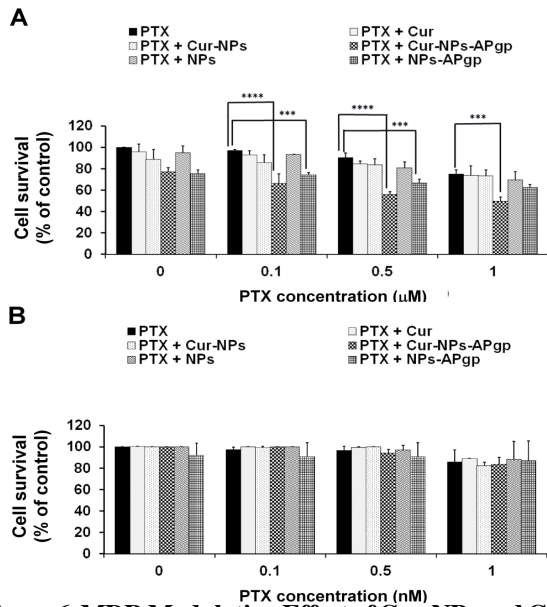


Figure 6. MDR Modulation Effect of Cur-NPs and Cur-NPs-APgp on PTX Sensitivity in KB-V1 and KB-3-1 Cells was Determined. The combined treatment of PTX with or without Cur, Cur-NPs, Cur-NPs-APgp, NPs or NPs-APgp was performed by pretreating the samples with Cur, Cur-NPs, Cur-NPs-APgp, NPs or NPs-APgp for 6 h, then treating them with various concentrations of PTX for an additional 42 h in KB-V1 (A) and KB-3-1 (B) cells. All assays were performed in triplicate and the mean±standard deviations are shown as *** $p < 0.001$ or **** $p < 0.0001$ versus PTX alone at each indicated concentration

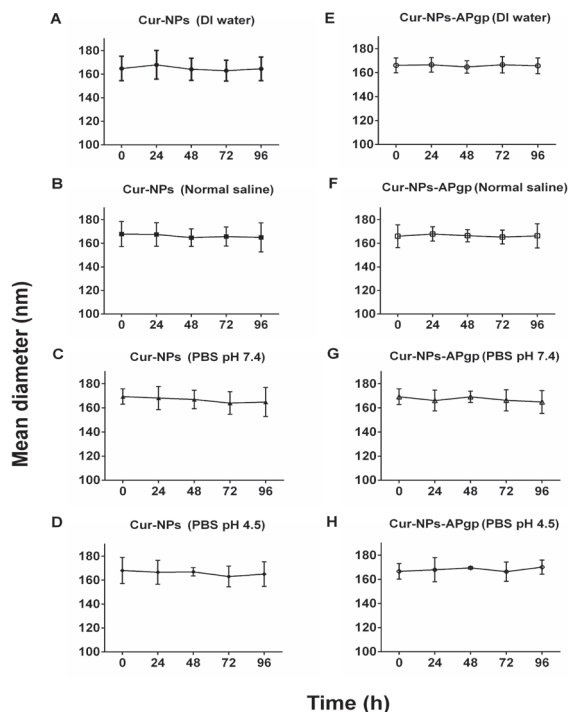


Figure 7. The Stability Testing of Cur-NPs (A-D) and Cur-NPs-APgp (E-H) was Performed to Investigate the Stability in the Mean Diameter of the NPs Over Time. The mean diameter of Cur-NPs and Cur-NPs-APgp in various solutions including DI water (A, E), normal saline (B, F), phosphate buffer saline (PBS) pH 7.4 (C, G) and pH 4.5 (D, H) at the indicated times were determined using PCS

Stability test of Cur-NPs and Cur-NPs-APgp

The Cur-NPs and Cur-NPs-APgp were stored at 4°C in various solutions including DI water, normal saline, phosphate buffer saline (PBS) pH 7.4 and pH 4.5 to study their short-term stability over time. The mean particle diameter was determined by PCS every day for 5 days to evaluate the aggregation of NPs. For the short-term stability test, the mean particle diameter of Cur-NPs and Cur-NPs-APgp at different time points and in various solutions showed a consistent size, proving their stability at 4°C in various storage solutions (Figure 7).

Discussion

MDR remains a critical reason for therapeutic failure in patients with various types of cancer, including cervical cancer. KB-V1 (human cervix carcinoma) cells highly express P-gp on the cell surface, which may efflux PTX out of the cells. The cancer cells could therefore survive due to a decrease in the intracellular concentration of PTX. We reported previously that Cur is a P-gp reversing agent, which reduces P-gp expression and function in KB-V1 cells *in vitro* (Anuchapreeda et al., 2002). Cur also enhances the sensitivity of many anti-cancer drugs, including vinblastine (Anuchapreeda et al., 2002; Chearwae et al., 2004; Limtrakul et al., 2004). The *in vitro* data (Figure 1) confirmed that Cur (5 and 7.5 μM) could enhance PTX sensitivity approximately 2.5- and 33.3-fold, respectively. Additionally, the present study is the first to show the *in vivo* MDR-reversing properties of Cur in a combined treatment with PTX. The increased accumulation of PTX following Cur pretreatment resulted in the induction of cell death, which caused an inhibition in tumor growth. Due to the poor solubility of Cur and its insolubility in water or saline (which are more compatible with humans and animals), the vehicle used was 3% DMSO and 1% Tween-20 in saline. Although this solution was not found to be toxic to animals, it may not be compatible with and applicable to humans. To develop the use of Cur as an adjuvant for cancer chemotherapy, we previously modified PLGA-NPs as a drug delivery system that may enhance Cur solubility (Punfa et al., 2012).

NPs have been associated with improvements in patient survival and quality of life by simultaneously increasing intracellular drug concentrations and reducing dose-limiting toxicity levels (Cho et al., 2008). Moreover, NPs could increase the solubility of a drug and enhance its safety and biocompatibility. The next generation of NP systems may target ligands, such as antibodies, peptides, or aptamers, which may further increase tumor specificity and cell internalization and will likely improve the treatment efficacy and decrease the serious side effects for many cytotoxic anti-neoplastic drugs (Zhang et al., 2008). In a previous study, a multifunctional mesoporous silica NP carrier was used to overcome Dox resistance in a multidrug-resistant human breast cancer xenograft by co-delivering Dox and siRNA, which target the P-glycoprotein drug transporter (Meng et al., 2013). Thus, the development of a combined treatment with a MDR reversing agent and conjugated NPs will be evaluated for its ability to overcome drug resistance in cancer patients.

Cur-NPs and Cur-NPs-APgp, in the range 150-180 nm with a narrow size distribution similar to our previous preparation (Punfa et al., 2012), were constructed and subjected to an *in vivo* pharmacokinetic study. The concentration of Cur in the serum of Cur-NPs- and Cur-NPs-APgp-treated mice was more prolonged than with free Cur. This may be due to the inherent properties of NPs, which may prevent the rapid metabolism of Cur, provide a sustained release, and change the drug pharmacokinetics to improve efficacy (Manjunath and Venkateswarlu, 2005; Zhang et al., 2008; Wang et al., 2012). These results were consistent with our previous *ex vivo* data from a Cur-releasing assay, which showed a sustained and prolonged release of Cur in the buffer for up to 10 days (Punfa et al., 2012).

The NPs also prevented the premature release of Cur or the chemotherapeutic drug, and thus reduced its nonspecific toxicity. Under physiological conditions, at an approximate pH value of 7.4, the release of any compound loaded in NPs is lower than in the acidic environment of the endosomes. Endocytosis of the NPs as endosomes catalyzes the release of the active compound, providing localized delivery inside the tumor cells (Kiziltepe et al., 2012). The present study observed that Cur could remain in circulation longer in the groups treated with Cur-NPs than in those treated with Cur-NPs-APgp, because the Cur-NPs were nonspecifically diffused whereas the Cur-NPs-APgp could directly target the tumor. The tissue distribution (in the liver and kidneys) of Cur was not detected, which may be due to the low dose of the Cur injection and the limited sensitivity of the HPLC method.

In our previous study, the biological effects of Cur-NPs were reported in terms of improving solubility and sustaining and prolonging the cumulative release of Cur when it was entrapped in NPs. Additionally, we have enhanced the specificity of the NPs to MDR cervical cancer cells that overexpressed P-gp by conjugation of the NPs with the APgp, which is known to function as an active-targeting drug delivery system. We found that Cur-NPs-APgp could enhance the cellular uptake and cytotoxicity of Cur in KB-V1 cells *in vitro* (Punfa et al., 2012).

In the present *in vivo* study, although NPs were prepared on a large scale, the actual loading of Cur was not different, while the entrapment efficiency slightly decreased when compared with the previous *ex vivo* study (Punfa et al., 2012). The decrease in the entrapment efficiency may be the result of a washing step that was administered during the NP preparation. Each new preparation of the NPs was reproducible. The freeze-dried NP preparation should be further studied and developed to improve the long-term stability of NPs and to optimize convenience for clinical use (Abdelwahed et al., 2006). A combined treatment of PTX with Cur-NPs-APgp reduced the tumor size when compared to the other groups, but was not statistically significant, possibly due to a large margin of error. However, the combined treatment of PTX with Cur-NPs had no effect on the tumor growth. This may be the effect of APgp on the NP surface, which could rapidly and specifically direct the NPs to target the MDR tumor cells.

The number of macrophages that accumulated in the livers of the combined treatment of PTX with the empty NPs or Cur-NPs-treated mice is one of the most important aspects of the data. Intravenous-injected NPs were rapidly recognized and sequestered by the reticuloendothelial system (RES), especially by macrophages, which compose the main population of the RES (Sadauskas et al., 2007; Ohara et al., 2012). Because only a few macrophages were detected in the livers of the Cur-NPs-APgp-treated mice, this suggests that Cur-NPs-APgp may not have been absorbed into the macrophages, but rather may have been absorbed by the tumor cells. Moreover, the APgp itself is a highly specific inhibitor of the P-gp-mediated MDR, and therefore could inhibit the efflux of PTX from the MDR cells and increase the cytotoxicity of PTX to induce cell death. Cur together with APgp might provide the synergistic effect of inhibiting P-gp function and enhancing the sensitivity of the MDR cancer cells to PTX. Therefore, we next confirmed this hypothesis *in vitro* by utilizing the MDR-reversing property of the NPs.

According to the data from the *in vitro* study, pretreatment with Cur-NPs-APgp was the most effective way to enhance PTX-induced cell death, while the survival of cells pretreated with Cur showed no difference when compared to PTX alone. These results suggested that APgp could bring Cur-NPs to the targeted KB-V1 cells and could inhibit P-gp function, resulting in enhanced PTX toxicity within a short time period. These results are consistent with the *in vivo* pharmacokinetic data, in which Cur was not detected in serum 60 min following an i.v. injection, as well as with our previous report showing that the internalization of Cur-NPs-APgp into KB-V1 cells was earlier than for Cur-NPs (Punfa et al., 2012). NPs-APgp slightly reduced cell survival, which suggests that APgp itself could inhibit P-gp function, leading to an enhancement of the cytotoxicity of PTX in the cells, similar to a previous study that reported the inhibition of P-gp function by different clones of APgp (Mechetner and Roninson, 1992). Taken together, Cur contained in the NPs and APgp on the NPs surface may provide a synergistic effect to increase PTX accumulation in the cells by inhibiting P-gp function.

Although Cur shows a high anti-cancer efficiency, it is limited due to poor solubility, which is an obstacle for any clinical application. However, the nanotechnology, especially the "active target drug delivery system," may improve the solubility and stability of Cur for its development as either an anti-cancer agent or an adjuvant therapy, which may enhance the efficacy of the anticancer drug in the MDR cancer treatment. A freeze-drying process was used for preserve the NPs for long-term stability testing. The stability of a PLGA nanoparticle prototype (NP and NP-anti-P-gp) that was encapsulated with coumarin has been studied (Iangcharoen et al., 2011). The size distribution between the non-freeze-dried-NPs and the freeze-dried-NPs was narrow, indicating that uniformity was maintained and aggregation did not occur after the freeze-drying process. Moreover, the cellular uptake of the NPs remained intact after the freeze-drying process (Yamate et al., 1993). Therefore, the freeze-dried coumarin-NPs and coumarin-encapsulated nanoparticles

conjugated with an anti-P-gp antibody that have a similar core structure to Cur-NPs and Cur-NPs-APgp, respectively, could be stored at 4°C for at least 1 month without any change in biological activity. In the present study, the short-term stability of the NPs was determined by observing the aggregation of NPs through measuring the mean particle diameter at different times and in various solutions. We found no difference in the mean diameter of the NPs in various solutions up to 5 days, indicating that no aggregations occurred in both Cur-NPs and Cur-NPs-APgp. These results demonstrated that the stability of the NPs maintained in various solutions at 4°C was a minimum of 5 days.

Overall, our study indicated that Cur-NPs-APgp could be the most effective way to enhance MDR cancer sensitivity to PTX *in vitro* and decrease tumor growth *in vivo* but not significantly due to the large margin of error. However, this may be a candidate for further research and development of Cur in nanotechnology applications to be used in the treatment of cancer patients, either as an MDR modulator or as a cancer treatment. Additionally, NPs-APgp may enhance MDR cancer sensitivity to PTX. To overcome MDR, NPs-APgp might therefore be one possible alternative carrier for the entrapment of anticancer drugs that are substrates of P-gp. For short-term stability, the NPs can be maintained in various solutions at 4°C for a minimum of 5 days without aggregation. However, the freeze-dried NPs preparation should be further studied and developed to improve the long-term stability of the NPs and to optimize convenience for clinical use.

Acknowledgements

The authors would like to acknowledge financial support from the Research, Development and Engineering (RD&E) Fund through The National Nanotechnology Center (NANOTEC), The National Science and Technology Development Agency (NSTDA), Thailand (Project P-12-01391) to Chiang Mai University, the Royal Golden Jubilee Ph.D. Program of Thailand and the Department of Experimental Pathology and Tumor Biology, Graduate School of Medical Science, Nagoya City University, Nagoya, Japan.

References

Abdelwahed W, Degobert G, Stainmesse S, Fessi H (2006). Freeze-drying of nanoparticles: formulation, process and storage considerations. *Adv Drug Deliv Rev*, **58**, 1688-713.

Anand P, Kunnumakkara AB, Newman RA, Aggarwal BB (2007). Bioavailability of curcumin: problems and promises. *Mol Pharm*, **4**, 807-18.

Anuchapreeda S, Leechanachai P, Smith MM, Ambudkar SV, Limtrakul PN (2002). Modulation of P-glycoprotein expression and function by curcumin in multidrug-resistant human KB cells. *Biochem Pharmacol*, **64**, 573-82.

Bain LJ, McLachlan JB, LeBlanc GA (1997). Structure-activity relationships for xenobiotic transport substrates and inhibitory ligands of P-glycoprotein. *Environ Health Perspect*, **105**, 812-8.

Burgio DE, Gosland MP, McNamara PJ (1998). Effects of P-glycoprotein modulators on etoposide elimination and

central nervous system distribution. *J Pharmacol Exp Ther*, **287**, 911-7.

Chang G (2003). Multidrug resistance ABC transporters. *FEBS Letters*, **555**, 102-5.

Chearwae W, Anuchapreeda S, Nandigama K, Ambudkar SV, Limtrakul P (2004). Biochemical mechanism of modulation of human P-glycoprotein (ABCB1) by curcumin I, II, and III purified from Turmeric powder. *Biochem Pharmacol*, **68**, 2043-52.

Cho K, Wang X, Nie S, Chen ZG, Shin DM (2008). Therapeutic nanoparticles for drug delivery in cancer. *Clin Cancer Res*, **14**, 1310-6.

CIOMS (1985). International guiding principles for biomedical research involving animals. *Altern Lab Anim*, **12**, 2.

Cirstoiu-Hapca A, Buchegger F, Lange N, et al (2010). Benefit of anti-HER2-coated paclitaxel-loaded immuno-nanoparticles in the treatment of disseminated ovarian cancer: Therapeutic efficacy and biodistribution in mice. *J Control Release*, **144**, 324-31.

Cisternino S, Rousselle C, Debray M, Scherrmann JM (2004). In situ transport of vinblastine and selected P-glycoprotein substrates: implications for drug-drug interactions at the mouse blood-brain barrier. *Pharm Res*, **21**, 1382-9.

Dai X-Z, Yin H-T, Sun L-F, et al (2013). Potential therapeutic efficacy of curcumin in liver cancer. *Asian Pac J Cancer Prev*, **14**, 3855-9.

Gallo JM, Li S, Guo P, Reed K, Ma J (2003). The effect of P-glycoprotein on paclitaxel brain and brain tumor distribution in mice. *Cancer Res*, **63**, 5114-7.

Hu YP, Pourquier P, Doignon F, Crouzet M, Robert J (1996). Effects of modulators of multidrug resistance on the expression of the MDR1 gene on human KB cells in culture. *Anticancer Drugs*, **7**, 738-44.

Iangcharoen P, Punfa W, Yodkeeree S, et al (2011). Anti-P-glycoprotein conjugated nanoparticles for targeting drug delivery in cancer treatment. *Arch Pharm Res*, **34**, 1679-89.

Jang SH, Wientjes MG, Au JL (2001). Kinetics of P-glycoprotein-mediated efflux of paclitaxel. *J Pharmacol Exp Ther*, **298**, 1236-42.

Kiziltepe T, Ashley JD, Stefanick JF, et al (2012). Rationally engineered nanoparticles target multiple myeloma cells, overcome cell-adhesion-mediated drug resistance, and show enhanced efficacy *in vivo*. *Blood Cancer J*, **2**, 64.

Lazzari S, Moscatelli D, Codari F, et al (2012). Colloidal stability of polymeric nanoparticles in biological fluids. *J Nanopart Res*, **14**, 920.

Limtrakul P, Khantamat O, Pintha K (2004). Inhibition of P-glycoprotein activity and reversal of cancer multidrug resistance by *Momordica charantia* extract. *Cancer Chemother Pharmacol*, **54**, 525-30.

Maeda H, Wu J, Sawa T, Matsumura Y, Hori K (2000). Tumor vascular permeability and the EPR effect in macromolecular therapeutics: a review. *J Control Release*, **65**, 271-84.

Makadia HK, Siegel SJ (2011). Poly lactic-co-glycolic acid (PLGA) as biodegradable controlled drug delivery carrier. *Polymers (Basel)*, **3**, 1377-97.

Manjunath K, Venkateswarlu V (2005). Pharmacokinetics, tissue distribution and bioavailability of clozapine solid lipid nanoparticles after intravenous and intraduodenal administration. *J Control Release*, **107**, 215-28.

Mechetner EB, Roninson IB (1992). Efficient inhibition of P-glycoprotein-mediated multidrug resistance with a monoclonal antibody. *Proc Natl Acad Sci U S A*, **89**, 5824-8.

Meng H, Mai WX, Zhang H, et al (2013). Codelivery of an optimal drug/siRNA combination using mesoporous silica nanoparticles to overcome drug resistance in breast cancer *in vitro* and *in vivo*. *ACS Nano*, **7**, 994-1005.

- Ohara Y, Oda T, Yamada K, et al (2012). Effective delivery of chemotherapeutic nanoparticles by depleting host Kupffer cells. *Int J Cancer*, **131**, 2402-10.
- Oyagbemi AA, Saba AB, Ibraheem AO (2009). Curcumin: from food spice to cancer prevention. *Asian Pac J Cancer Prev*, **10**, 963-7.
- Punfa W, Yodkeeree S, Pitchakarn P, Ampasavate C, Limtrakul P (2012). Enhancement of cellular uptake and cytotoxicity of curcumin-loaded PLGA nanoparticles by conjugation with anti-P-glycoprotein in drug resistance cancer cells. *Acta Pharmacol Sin*, **33**, 823-31.
- Qiao WJ, Cheng HY, Li CQ, et al (2011). Identification of pathways involved in paclitaxel activity in cervical cancer. *Asian Pac J Cancer Prev*, **12**, 99-102.
- Qureshi S, Shah AH, Ageel AM (1992). Toxicity studies on *Alpinia galanga* and *Curcuma longa*. *Planta Med*, **58**, 124-7.
- Sadauskas E, Wallin H, Stoltenberg M, et al (2007). Kupffer cells are central in the removal of nanoparticles from the organism. *Part Fibre Toxicol*, **4**, 10.
- Shehzad A, Wahid F, Lee YS (2010). Curcumin in cancer chemoprevention: molecular targets, pharmacokinetics, bioavailability, and clinical trials. *Arch Pharm*, **343**, 489-99.
- Shen F, Chu S, Bence AK, et al (2008). Quantitation of doxorubicin uptake, efflux, and modulation of multidrug resistance (MDR) in MDR human cancer cells. *J Pharmacol Exp Ther*, **324**, 95-102.
- Song Z, Feng R, Sun M, et al (2011). Curcumin-loaded PLGA-PEG-PLGA triblock copolymeric micelles: Preparation, pharmacokinetics and distribution *in vivo*. *J Colloid Interface Sci*, **354**, 116-23.
- Tabatabaei Mirakabad FS, Nejati-Koshki K, Akbarzadeh A, et al (2014). PLGA-Based Nanoparticles as Cancer Drug Delivery Systems. *Asian Pac J Cancer Prev*, **15**, 517-35.
- Torchilin VP (2005). Recent advances with liposomes as pharmaceutical carriers. *Nat Rev Drug Discov*, **4**, 145-60.
- Tsai YM, Chien CF, Lin LC, Tsai TH (2011). Curcumin and its nano-formulation: the kinetics of tissue distribution and blood-brain barrier penetration. *Int J Pharm*, **416**, 331-8.
- Wang W, Zhu R, Xie Q, et al (2012). Enhanced bioavailability and efficiency of curcumin for the treatment of asthma by its formulation in solid lipid nanoparticles. *Int J Nanomedicine*, **7**, 3667-77.
- Yadav D, Anwar MF, Garg V, et al (2014). Development of polymeric nanopaclitaxel and comparison with free paclitaxel for effects on cell proliferation of MCF-7 and B16F0 carcinoma cells. *Asian Pac J Cancer Prev*, **15**, 2335-40.
- Yamate J, Tatsumi M, Nakatsuji S, et al (1993). Immunohistochemical observations of macrophages and perisinusoidal cells in carbon tetrachloride-induced rat liver injury. *J Vet Med Sci*, **55**, 973-7.
- Yin H-T, Zhang D-G, Wu X-L, Huang X-E, Chen G (2013). *In vivo* evaluation of curcumin-loaded nanoparticles in a A549 xenograft mice model. *Asian Pac J Cancer Prev*, **14**, 409-12.
- Zhang C, Qu G, Sun Y, et al (2008). Pharmacokinetics, biodistribution, efficacy and safety of N-octyl-O-sulfate chitosan micelles loaded with paclitaxel. *Biomaterials*, **29**, 1233-41.
- Zhang L, Gu FX, Chan JM, et al (2008). Nanoparticles in medicine: therapeutic applications and developments. *Clin Pharmacol Ther*, **83**, 761-9.